

Protonation States of Buried Histidine Residues in Human Deoxyhemoglobin Revealed by Neutron Crystallography

Toshiyuki Chatake,[†] Naoya Shibayama,[‡] Sam-Yong Park,[§] Kazuo Kurihara,[¶] Taro Tamada,[¶] Ichiro Tanaka,[#] Nobuo Niimura,[#] Ryota Kuroki,[¶] and Yukio Morimoto^{*†}

Research Reactor Institute, Kyoto University, Kumatori, Osaka 590-0494, Japan, Department of Physiology, Jichi Medical University, Shimotsuke, Tochigi 329-0498, Japan, Protein Design Laboratory, Yokohama City University, Tsurumi, Yokohama 230-0045, Japan, Quantum Beam Science Directorate, Japan Atomic Energy Agency, Tokai, Ibaraki 319-1195, Japan, and Department of Technology, Ibaraki University, Hitachi, Ibaraki 316-8511, Japan

Received July 4, 2007; E-mail: morimoto@rri.kyoto-u.ac.jp

Human hemoglobin (Hb), an $\alpha_2\beta_2$ tetrameric hemoprotein arranged as a dimer of identical $\alpha\beta$ dimers, has evolved to allow efficient transport of oxygen from the lungs to tissues. Perhaps the most remarkable property of Hb is cooperativity that is generally explained as the result of a shift in the equilibrium between the two quaternary structures from the low-affinity T (tense) state to the high-affinity R (relaxed) state during oxygenation.¹ However, the binding of oxygen to Hb is further modulated by protons, chloride ions, and inorganic phosphate that preferentially stabilize the T state and facilitate the release of oxygen from Hb when it reaches the tissues.² Much of our knowledge of the control mechanisms of Hb is based on the X-ray crystal structures of T-state deoxyhemoglobin (deoxyHb) and R state oxyhemoglobin (oxyHb). However, the invisibility of hydrogen (H) atoms in X-ray crystallography has hindered the direct visualization of the proton distribution of Hb in each allosteric state. Neutron crystallographic analysis can locate the H atoms even at medium resolution.³ Here we present the first neutron crystal structure of human deoxyHb. Our structure reveals unexpected protonation states of some buried histidine residues, including distal histidine residues in both subunits, and provides new insight into the mechanisms of pH-dependent control of oxygen affinity.

A large crystal of human adult deoxyHb ($4 \times 3 \times 3 \text{ mm}^3$) grown from D_2O solution (pD 6.3) was used for neutron diffraction experiments (Supporting Information). The preliminary experiment was carried out at the KUR reactor in RRI of Kyoto University, and the diffraction data set to 2.1 Å resolution was collected at JRR-3M reactor in JAEA using the BIX-3 diffractometer.⁴ Since all labile H atoms (either N- or O-linked) have been replaced by deuterium (D) atoms during crystallization in D_2O solution, protonation can be identified as positive peaks near the $\text{N}_{\delta 1}$ and $\text{N}_{\epsilon 2}$ atoms of histidines (Supporting Information). In this study, the protonation of 10 ordered histidines out of the total 19 histidines (per $\alpha\beta$ dimer) was determined by the strong positive densities ($> +2.5\sigma$) at D positions in omit $|F_o| - |F_c|$ maps, in which all the histidines had not been included in the initial model (Table 1). Because the protonation states of these histidines are very similar between each of the crystallographically independent α and β subunits, the α_1 and β_1 subunits are selected for presentation in the results and figures.

Figure 1 shows neutron $2|F_o| - |F_c|$ Fourier maps for vicinities of the α - and β -heme groups of deoxyHb at pD 6.3. For the heme-

Table 1. Statistics Regarding the Protonation States of 10 Ordered Histidine Residues in Human Deoxyhemoglobin^a

residue	in $\alpha_1\beta_1$ dimer	in $\alpha_2\beta_2$ dimer	note
$\alpha 45$	$\text{D}_{\epsilon 2}(3.5)$	$\text{D}_{\epsilon 2}(3.3)$	
$\alpha 58$	$\text{D}_{\delta 1}(3.6), \text{D}_{\epsilon 2}(3.3)$	$\text{D}_{\delta 1}(3.3), \text{D}_{\epsilon 2}(3.9)$	distal histidine
$\alpha 72$	$\text{D}_{\epsilon 2}(3.5)$	$\text{D}_{\epsilon 2}(3.3)$	
$\alpha 87$	$\text{D}_{\delta 1}(4.2)$	$\text{D}_{\delta 1}(4.2)$	proximal histidine
$\alpha 103$	$\text{D}_{\delta 1}(4.2), \text{D}_{\epsilon 2}(4.4)$	$\text{D}_{\delta 1}(4.3), \text{D}_{\epsilon 2}(4.4)$	$\alpha_1\beta_1/\alpha_2\beta_2$ contact
$\alpha 112$	$\text{D}_{\epsilon 2}(4.7)$	$\text{D}_{\epsilon 2}(3.5)$	
$\alpha 122$	$\text{D}_{\epsilon 2}(4.5)$	$\text{D}_{\epsilon 2}(3.4)$	$\alpha_1\beta_1/\alpha_2\beta_2$ contact
$\beta 63$	$\text{D}_{\delta 1}(3.1), \text{D}_{\epsilon 2}(2.8)$	$\text{D}_{\delta 1}(2.8), \text{D}_{\epsilon 2}(3.6)$	distal histidine
$\beta 92$	$\text{D}_{\delta 1}(3.8)$	$\text{D}_{\delta 1}(4.4)$	proximal histidine
$\beta 116$	$\text{D}_{\delta 1}(3.4), \text{D}_{\epsilon 2}(4.1)$	$\text{D}_{\delta 1}(3.2), \text{D}_{\epsilon 2}(3.8)$	$\alpha_1\beta_1/\alpha_2\beta_2$ contact

^a Values in parentheses are for peak height for D positions.

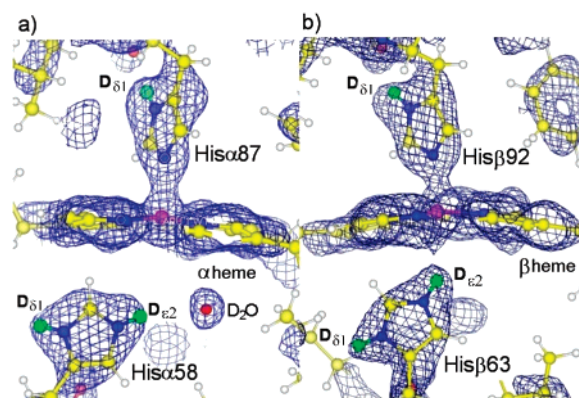


Figure 1. Refined $2|F_o| - |F_c|$ neutron Fourier maps superimposed on the ball-and-stick model around the (a) α_1 heme and (b) β_1 heme. The plane of each heme group is placed perpendicular to the paper. The blue contours show $+1.5\sigma$ densities. The elements are colored white, green, yellow, blue, red, and purple for H, D, C, N, O, and Fe atoms, respectively.

linked proximal histidines, His α 87 and His β 92, there is a strong positive density at the $\text{D}_{\delta 1}$ position, consistent with $\text{N}_{\delta 1}$ being protonated, whereas $\text{N}_{\epsilon 2}$ is bonded to the heme iron. However, the protonation states of distal histidines are unexpected. Both distal histidines, His α 58 and His β 63, adopt a positively charged, fully (doubly) protonated form, as evidenced by well-defined positive densities at both $\text{D}_{\delta 1}$ and $\text{D}_{\epsilon 2}$ positions (Figure 1 and Table 1). This finding sharply contrasts with existing results on R state liganded Hbs where such full protonation can never occur. For example, a heteronuclear NMR study of CO-bound Hb at pH 6.5 shows that both distal histidines exist in the neutral $\text{N}_{\epsilon 2}$ -H tautomer, deprotonated at $\text{N}_{\delta 1}$ atoms.⁵ The same is true for oxyHb.⁵ From these data taken together, we find that the pK_a values of distal histidines are markedly higher in deoxyHb than in liganded Hbs. This previously

[†] Kyoto University.

[‡] Jichi Medical University.

[§] Yokohama City University.

[¶] Japan Atomic Energy Agency.

[#] Ibaraki University.

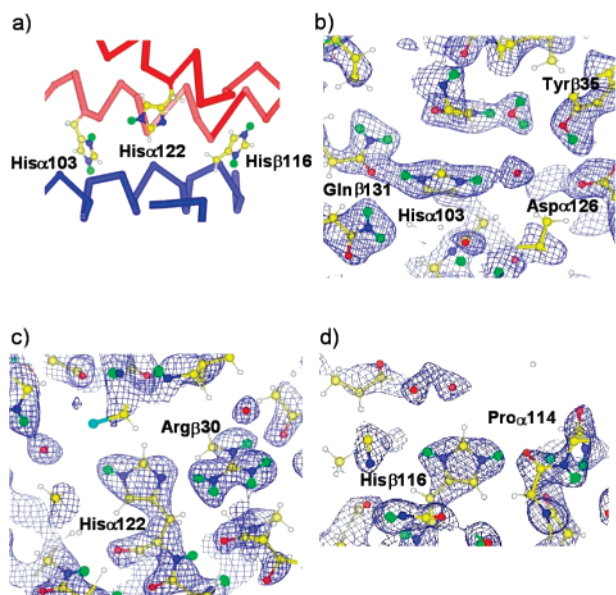


Figure 2. Histidine residues at the $\alpha_1\beta_1$ interface: (a) the schematic diagram showing the locations of these three histidine residues. Red and blue sticks indicate C_α backbone of α_1 and β_1 subunits, respectively. (b–d) Neutron $2|F_o|-|F_c|$ Fourier maps contoured at 1.5σ level around (b) His α 103, (c) His α 122, and (d) His β 116 in the $\alpha_1\beta_1$ dimer.

unrecognized pK_a change is of physiological relevance because it ensures that both the α - and β -distal histidines play a certain role in the Bohr effect of Hb.

The finding of fully protonated distal histidines is also in contrast to available neutron data on aquomet- and CO-bound forms of sperm whale myoglobin (Mb).⁶ In either form of Mb, the distal histidine was in the N_{δ_1} -H tautomer, stabilized by a H-bond between N_{δ_1} -D δ_1 and a sulfate/water molecule (aquomet/CO-bound) located in the heme pocket. Moreover, previous NMR titration and X-ray crystallographic studies indicate that the Mb distal histidine is neutral at pH above 4.77 and should not be fully protonated without local structural changes to the heme pocket.⁸

The neutron structure also reveals the protonation states of the other three buried histidine residues, His α 103, His α 122, and His β 116, which are located across the intradimeric $\alpha_1\beta_1$ contact of Hb (Figure 2a and Table 1). Of the three, the two α subunit histidines, His α 103 and His α 122, are completely buried within the $\alpha_1\beta_1$ interface and have been suggested to have very low pK_a values (<5.6) in both deoxy- and CO-bound Hb.⁹ Our structure shows, however, that His α 103 is doubly protonated and acts as a H-bond donor, which is capable of satisfactorily connecting the α_1 and β_1 subunits (Figure 2b): N_{ϵ_2} -D ϵ_2 forms a H-bond to the side-chain carbonyl of Gln β 131, and N_{δ_1} -D δ_1 makes a water-mediated H-bonding network connecting the hydroxyl group of Tyr β 35, the carboxyl group of Asp α 126, and the N_{ϵ_2} -D ϵ_2 group of His α 122. On the other hand, as expected, His α 122 exists in the N_{ϵ_2} -D ϵ_2 tautomer: N_{ϵ_2} -D ϵ_2 forms a water-mediated H-bond with the hydroxyl group of Tyr β 35, and deprotonated N_{δ_1} is able to make a close contact with the guanidinium group of Arg β 30 by H-bond (Figure 2c). We also found that partially exposed His β 116 (near the edge of the $\alpha_1\beta_1$ interface) is doubly protonated, with its N_{ϵ_2} -D ϵ_2 group H-bonding to the main-chain carbonyl of Pro α 114 (Figure 2d). Overall, these neutron data provide the most accurate picture of the $\alpha_1\beta_1$ H-bonding network in deoxyHb as ever reported and allow us to observe unambiguously the nature of the intradimeric interactions at an atomic level.

The protonation states of specific histidines in Hb have long been a topic of interest to many investigators for nearly 100 years since

they are related to the mechanisms of the alkaline Bohr effect. Two factors are known to contribute to the full expression of the alkaline Bohr effect of Hb, namely, the release of protons associated with quaternary structural transition from the T state to the R state, and those associated with oxygen binding by the T state of Hb, the so-called “T-state Bohr effect” (or tertiary Bohr effect within the T state). The former factor has been correlated to the imidazole groups of surface histidines such as His β 146, His α 20, and His α 89, and other proton binding site (e.g., the α -amino group of Val α 1), whose pK_a values fall in the physiological pH range but differ between the T and R conformation of Hb.¹⁰ On the other hand, the T-state Bohr effect is only addressed briefly for lack of information about local tertiary structural changes within the T quaternary structure.^{2a} Our present results suggest an interesting possibility that both the α - and β -distal histidines, His α 58 and His β 63, could contribute to the T-state Bohr effect of Hb. Indeed, the protonation/deprotonation of each distal histidine may have a direct impact on the oxygen affinity of the nearby heme group through sterical hindrance and/or polarity change in the heme pocket without affecting the allosteric equilibrium of Hb.

In conclusion, the neutron crystal structure of human deoxyHb reveals that both the α - and β -distal histidines (His α 58 and His β 63) adopt a positively charged, fully (doubly) protonated form, suggesting their contribution to the T-state Bohr effect of Hb. In addition, this study demonstrates the power of neutron crystallography to better define intersubunit H-bonding networks of large oligomeric proteins.

Acknowledgment. This work was supported in part by a Grant-in-Aid for Scientific Research from the Ministry of Education, Culture, Sports, Science and Technology of Japan (No. 17053011 to Y.M.), the REIMEI Research Resources of Japan Atomic Energy Research Institute (to Y.M.), and Hyogo Science and Technology (to Y.M.).

Supporting Information Available: Experimental details, data statistics, and a complete table of neutron densities for protonation sites of all histidine residues in deoxyHb. This material is available free in charge via Internet at <http://pubs.acs.org>.

References

- (1) (a) Gelin, B. R.; Lee, A. W.; Karplus, M. *J. Mol. Biol.* **1983**, *25*, 489–559. (b) Monod, J.; Wyman, J.; Changeux, J. P. *J. Mol. Biol.* **1965**, *12*, 88–118. (c) Park, S.-Y.; Yokoyama, T.; Shibayama, N.; Shiro, Y.; Tame, J. R. H. *J. Mol. Biol.* **2006**, *360*, 690–701.
- (2) (a) Pertuz, M. F.; Wilkinson, A. J.; Paoli, M.; Dodson, G. G. *Annu. Rev. Biophys. Biomol. Struct.* **1998**, *27*, 1–34. (b) Imai, K. *Allosteric Effects in Haemoglobin*; Cambridge University Press: London, 1982.
- (3) (a) Helliwell, J. R. *Nat. Struct. Biol.* **1997**, *4*, 874–876. (b) Niimura, N. *Curr. Opin. Struct. Biol.* **1999**, *9*, 602–608. (c) Tsyba, I.; Bau, R. *Chemtracts* **2002**, *15*, 233–257. (d) Schoenborn, B. P.; Langan, P. J. *Synchrotron Radiat.* **2004**, *11*, 80–82.
- (4) Tanaka, I.; Kurihara, K.; Chatake, T.; Niimura, N. *J. Appl. Crystallogr.* **2002**, *35*, 34–40.
- (5) Lukin, J. A.; Simplaceanu, V.; Zou, M.; Ho, N. T.; Ho, C. *Proc. Natl. Acad. Sci. U.S.A.* **2000**, *97*, 10354–10358.
- (6) (a) Cheng, X. D.; Schoenborn, B. P. *J. Mol. Biol.* **1991**, *220*, 381–399. (b) Shu, F.; Ramakrishnan, V.; Schoenborn, B. P. *Proc. Natl. Acad. Sci. U.S.A.* **2000**, *97*, 3872–3877. (c) Ostermann, A.; Tanaka, I.; Engler, N.; Niimura, N.; Parak, F. G. *Biohyph. Chem.* **2002**, *95*, 183–193.
- (7) (a) Cocco, M. J.; Kao, Y. H.; Phillips, A. T.; Lecomte, J. T. *Biochemistry* **1992**, *31*, 6481–6491. (b) Bashford, D.; Case, D. A.; Dalvit, C.; Tennant, L.; Wright, P. E. *Biochemistry* **1993**, *32*, 8045–8056.
- (8) Yang, F.; Phillips, G. N., Jr. *J. Mol. Biol.* **1996**, *256*, 762–774.
- (9) Mihailescu, M. R.; Russu, M. *Proc. Natl. Acad. Sci. U.S.A.* **2001**, *98*, 3773–3777.
- (10) (a) Perutz, M. F.; Muirhead, H.; Mazzarella, L.; Crowther, R. A.; Greer, J.; Kilmartin, J. V. *Nature* **1969**, *222*, 1240–1243. (b) Ho, C.; Russu, I. M. *Biochemistry* **1987**, *26*, 6299–6305. (c) Sun, D. P.; Zou, M.; Ho, N. T.; Ho, C. *Biochemistry* **1997**, *36*, 6663–6673.

JA0749441